Infrared-Induced Isomerization of Ethanol Dimers Trapped in Argon and Nitrogen Matrices: Monochromatic Irradiation Experiments and DFT Calculations

S. Coussan

Department of Chemistry and Biochemistry, University of Bern, Freiestrasse 3, CH3000, Bern 9, Switzerland

M. E. Alikhani and J. P. Perchard*

LADIR/Spectrochimie Moléculaire, CNRS UMR 7075, Université Pierre et Marie Curie, case courrier 49, 4 Place Jussieu, 75252 Paris Cedex 05, France

W. Q. Zheng

LURE, Bâtiment 209D, Université Paris-Sud, 91405 Orsay Cedex, France

Received: January 10, 2000; In Final Form: March 23, 2000

Selective vibrational excitations of OH stretching modes of ethanol dimers trapped in solid argon or nitrogen were carried out in the range 3550−3500 cm^{-1}. This proved an efficient means to interconvert these dimers and thus to characterize several conformers by their most specific vibrational modes. The structures, energies, and vibrational properties of four minima of the potential energy surface have been investigated by the density functional method. These minima correspond to an open chain dimer where both proton donor (PD) and proton acceptor (PA) subunits are either *anti*- or *gauche*-ethanol, with well-differentiated vibrational spectra in the domains 1400−1240 and 1100−1020 cm^{-1}. The comparison between calculated and observed spectra in these domains enables the anti or gauche character of both PD and PA to be distinguished. In argon matrix four dimeric species were identified after deposition. All of them are sensitive to irradiation at the νOH frequency of their PD moiety, with simple conversion schemes for two of them. On one hand, the most abundant one, characterized by νOH bands at 3660.1 and 3527.2 cm^{-1}, is found to be anti−anti. Upon irradiation at 3527 cm^{-1}, it is converted into an unstable gauche−gauche form, not present before irradiation, which spontaneously reconverts into its precursor in the dark. On the other hand, another conformer with νOH frequencies at 3665.4−3536.2 cm^{-1}, also anti−anti, is converted upon irradiation at 3536 cm^{-1} into a new form whose identification is rendered difficult by the small number of bands assigned. In nitrogen not less than seven νOH bands in the range 3520−3470 cm^{-1} are assignable to dimers. Irradiations at various νOH PD frequencies are very efficient to interconvert these species whose structures are discussed on the same grounds as in the case of argon matrix. However the greater complexity of the conversion processes precludes a full assignment of the spectra except for the most abundant species for which the data are complete enough to conclude an anti−gauche structure.

I. Introduction

In some recent works relating to methanol aggregates,[1−5] we have shown that infrared photoisomerization in matrices is a powerful method for identifying the vibrational spectra of small clusters, from which structural information is inferred. This method is comparable to molecular beam depletion spectroscopy, also based on intermolecular bond breaking upon vibrational excitation. Its main advantage is a nearly complete assignment of the infrared spectra of the selectively photoisomerized cluster and of its photoinduced descendants, which are generally metastable conformers with lifetimes that are strongly temperature dependent.

The results described in this paper are an extension of the photoisomerization study of the methanol dimer trapped in Ar[4] and N_2[1,5] in the case of ethanol. For this molecule the existence of an internal rotation axis (C−O bond) suggests the possibility of a large number of conformers differing not only by the orientation of the two partners with respect to the O−H···O intermolecular axis, as for $(CH_3OH)_2$, but also by their local symmetry (C_s or C_1).[6] This conclusion was reached by Ehbrecht and Huisken[7] who have studied the dissociation of $(C_2H_5OH)_2$ formed in a jet upon excitation of its CCO stretching modes located between 1100 and 1000 cm^{-1}. The presence of six peaks of photodepletion between 1090 and 1030 cm^{-1} gives evidence for the existence of several conformers whose structures were discussed on the basis of semiempirical calculations. Three conformers, anti−gauche, anti−anti, and gauche−gauche, with comparable energies were calculated to be the forms experimentally observed. These results prompted us to carry out selective irradiation experiments in the 2.8 μm region under the same conditions as in the case of $(CH_3OH)_2$.[4,5] Comparable results were readily obtained in nitrogen matrix, while in argon greater conversion yields enabled the conformers involved in the conversion to be well-identified. Their structures were discussed on the basis of DFT calculations, which have been shown to provide reliable information about the structure and vibrational properties of hydrogen-bonded aggregates.[2,4,8−13] Accordingly this paper is organized in two parts. The first one

10.1021/jp0001283 CCC: $19.00 © 2000 American Chemical Society
Published on Web 05/23/2000

TABLE 1: Geometrical Parameters (r, Å; α, τ, ω, deg) of the Stable Forms of Ethanol Monomer and Dimers

	anti-ethanol					gauche-ethanol				
		dimer					dimer			
		PD		PA			PD		PA	
	monomer	a−a	a−g	a−a	g−a	monomer	g−g	g−a	g−g	a−g
*r*CC	1.515	1.512	1.517	1.514	1.514	1.521	1.524	1.523	1.519	1.519
*r*CO	1.432	1.424	1.424	1.441	1.441	1.429	1.423	1.423	1.438	1.438
*r*OH	0.960	0.969	0.969	0.961	0.961	0.961	0.969	0.969	0.962	0.962
*r*CH methylene[a]	1.095	1.096	1.096	1.093	1.093	[1.095 1.089	[1.096 1.090	[1.093 1.088	[1.093 1.088	[1.093 1.088
αCCO	108.0	108.6	108.6	108.2	108.3	112.9	113.0	1131	112.3	112.8
αCOH	109.1	109.2	109.3	109.0	108.9	108.8	109.2	109.1	108.8	108.8
τCCOH	180	178.5	179.0	178.4	179.1	61.9	66.9	67.8	59.9	60.1
*r*O···O		2.900	2.887	2.900	2.912		2.897	2.912	2.897	2.887
ωCC···CC		74.9	31.9	74.9	36.0		130.8	36.0	130.8	31.9

[a] For *gauche*-ethanol the first value refers to CH_1, the second to CH_2 (see Figure 1).

presents the DFT results for four stable dimeric forms for which a straightforward correlation between the effect of hydrogen bonding on the structural properties and the spectrum of each partner, already reported for $(CH_3OH)_2$,[4,9] can be established. The second one describes the experimental data, in particular the effects of selective irradiation from which the vibrational spectra of several conformers are well-identified. The comparison with DFT predictions enables then the anti or gauche character of each proton donor (PD) or proton acceptor (PA) subunit to be specified for some of them.

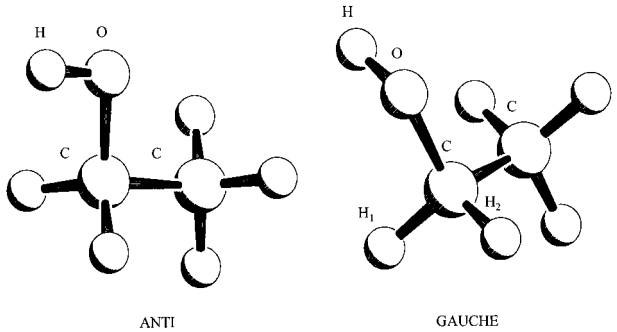

Figure 1. Two stable forms of ethanol monomer.

II. Experimental Section

The matrix experiments were carried out in two laboratories, in Paris and Orsay, using two different devices. In Paris we used a closed cycle helium cryostat (Air Products CSW 202) coupled to a Bruker 120 interferometer and, in Orsay, a liquid helium cryostat (L'Air Liquide) coupled to a Mattson-unicam Research Series II interferometer. In both cases the gas mixtures were prepared by standard manometric technique and sprayed on a Ni- or Au-plated Cu block cooled to 17 K (N_2) or 20 K (Ar). The deposition rate was varied between 5 and 10 mmol·h^{-1}. The spectra were recorded at about 7 K at 0.1 cm^{-1} (Paris) and 0.25 cm^{-1} (Orsay) resolution. Irradiations in the 3 μm region were performed in Orsay using a homemade optical parametric oscillator (OPO) previously described in ref 3. The average power was 25 mW and the line width of the order 1 cm^{-1}.

Natural ethanol (Prolabo, RP grade) was dried over sodium and distilled under vacuum. Argon and nitrogen matrix gases (L'Air liquide, N55 purity) were used without any further purification.

III. Theoretical Calculations on Ethanol Dimer

Density functional calculations were carried out using the Gaussian 98/DFT suite of programs[14] and the 6-311++G(2d,2p) basis set. The calculations employ the Becke3LYP nonlocal exchange correlation functional[15] previously used in studies of water,[8] methanol,[2,4,6,10−12] and ethanol[13] clusters.

For the monomer the two stable structures (anti and gauche) are displayed in Figure 1, and the corresponding geometrical parameters are reported in Table 1.

For the dimer full-geometry optimizations were performed for four minima as established by the absence of any imaginary vibrational frequencies. They correspond to open chain dimers, anti−anti, anti−gauche, gauche−anti, and gauche−gauche, the first term referring to PD, the second to PA. The dissociation energy (D_0) for these dimers was calculated as

$$D_0 = 2E(\text{monomer}) - E(\text{dimer})$$

where the terms *E*(monomer) and *E*(dimer) include the corresponding ZPE and BSSE corrections. The values follow the order anti−gauche (14.7) > gauche−gauche (14.2) > anti−anti (13.7) > gauche−anti (13.1) (values in kJ mol^{-1}). These relative stabilities are at variance with the results of Gonzáles et al.[13] who found the anti−anti form to be the most stable (D_0 = 15.1 kJ mol^{-1}), despite the use of the DFT method in both calculations. The difference probably arises from a more polarized (use of df orbitals for C and O atoms) but less diffuse basis set in ref 13 than in this work. Anyway the energies are so close to each other that their differences are not significative, leading to the conclusion that the potential energy surface is remarkably flat. This is the reason the relative stabilities found by Ehbrecht and Huisken,[7] anti−gauche > anti−anti > gauche−gauche, using a semiempirical potential are still different from the DFT results. The small energy differences between the four stable forms suggest the possibility of trapping anyone in low-temperature matrices, the matrix−dimer interaction being of same order of magnitude as these differences. Furthermore one may reasonably expect easy interconversions—either of photochemical or of thermal origin.

Table 1 gathers the geometrical properties of the four dimeric forms. The parameters relative to the anti conformer are reported in the left part, those relative to the gauche conformer in the right part. The usual effects of hydrogen bonding on the PA and PD subunits are well-identified for both anti and gauche conformers: for PD, shortening of *r*CO, lengthening of *r*CH (methylene) and *r*OH; for PA, lengthening of *r*CO and *r*OH and shortening of *r*CH (methylene). These changes in bond length, which agree with those reported in ref 13, are correlated

TABLE 2: Calculated Harmonic Vibrational Frequencies (cm^{-1}) of the Monomer and Frequency Shifts $\nu_{dimer}-\nu_{monomer}$ of Some Vibrational Modes of the Anti Form of Ethanol[a]

		PD		PA	
	monomer	anti−anti	anti−gauche	anti−anti	gauche−anti
νOH	3847.8 (29)	−163.6 (534)	−167.3 (542)	−7.4 (39)	−8.1 (39)
$\nu_a CH_2$	3016.4 (45)	−19.5 (51)	−18.6 (51)	26.0 (26)	25.5 (28)
$\nu_s CH_2$	2992.1 (65)	−15.1 (69)	−14.0 (71)	20.2 (59)	19.6 (60)
δOH	1270.5 (66)	57.1 (75)	55.8 (105)	5.6 (76)	6.7 (67)
$rCH_3 + \nu_a CCO$	1095.7 (22)	17.1 (24)	17.8 (22)	−9.3 (15)	−9.2 (29)
$\nu_a CCO + rCH_3$	1029.3 (70)	21.2 (78)	21.0 (40)	6.0 (85)	5.7 (78)
$\nu_s CCO$	894.4 (14)	3.7 (11)	4.0 (11)	−5.7 (24)	−5.9 (19)
$r CH_2 + rCH_3$	822.2 (0.3)	−3.3 (0.0)	−2.7 (0.0)	5.4 (0.4)	4.4 (0.4)

[a] Infrared intensities in km mol^{-1} reported in parentheses.

TABLE 3: Calculated Harmonic Vibrational Frequencies (cm^{-1}) of the monomer and frequency shifts ν_{dimer} - $\nu_{monomer}$ of Some Vibrational Modes of *gauche*-Ethanol[a]

		PD		PA	
	monomer	gauche−gauche	gauche−anti	gauche−gauche	anti−gauche
νOH	3832.6 (23)	−157.0 (456)	−150.4 (453)	−5.8 (31)	−5.8 (31)
$\nu_a CH_2$	3073.0 (4)	−9.6 (14)	−9.6 (16)	7.5 (9)	7.2 (9)
$\nu_s CH_2$	2998.8 (59)	−11.6 (71)	−14.9 (71)	22.6 (52)	22.7 (55)
$wCH_2 + \delta$OH + $\delta_s CH_3$	1419.3 (36)	19.5 (42)	20.5 (45)	3.3 (62)	4.5 (31)
$\delta_s CH_3 + wCH_2$	1407.0 (7)	3.5 (12)	3.8 (12)	4.3 (5)	4.3 (13)
$twCH_2 + \delta$OH	1373.1 (3)	21.1 (1)	21.9 (2)	−2.5 (2)	−2.2 (2)
$wCH_2 + \delta$OH + rCH_3	1282.6 (11)	16.9 (12)	17.8 (12)	0.4 (11)	0.3 (10)
$rCH_3 + \nu_a CCO$	1068.2 (97)	36.4 (81)	37.6 (68)	4.5 (75)	4.0 (67)
$\nu_a CCO + rCH_3$	1055.9 (31)	4.8 (56)	5.3 (53)	−6.0 (64)	−6.3 (116)
$\nu_s CCO$	880.8 (13)	3.0 (8)	2.6 (14)	−2.1 (24)	−1.7 (22)
$rCH_2 + rCH_3$	806.6 (3)	1.1 (2)	1.0 (2)	3.9 (9)	3.3 (5)

[a] Infrared intensities in km mol^{-1} reported in parentheses.

to the frequency shifts of the corresponding stretching modes. Tables 2 and 3 gather the data of particular relevance to the structural analysis of the dimer (the full sets of vibrational frequencies and intensities are available from the authors upon request). Each table is devoted to one conformer of ethanol, to emphasize the fact that the spectral response of each moiety depends only on its PA or PD role and on its own anti or gauche character and not on the conformation of its partner. This property simply stems from the absence of vibrational coupling between the two moieties and from a hydrogen-bonding strength nearly independent of the conformation of the two partners. For PD, the *r*CO shortening corresponds to a blue shift with respect to the monomer frequency of the three modes involving a contribution of νCO in the range 1100−880 cm^{-1} while νOH and νCH_2 are significantly red shifted, the corresponding bond length increasing by about 0.008 Å in both cases. For PA, the changes in bond length are opposite to those of PD for *r*CO and *r*CH (methylene) so that the corresponding frequencies are, respectively, red and blue shifted. As for νOH, its red shift of about 10 cm^{-1} correlates with a *r*OH increase of the order of 10^{-3} Å. An exception to the vibrational decoupling between PA and PD is noted in the case of the anti−gauche structure. It will be discussed below.

Figures 2−6 schematize the spectral properties of PA and PD according to their anti or gauche character in the discriminatory domains 1430−1230, 1100−1020, and 830−800 cm^{-1}. Figures 2 and 3 compare the calculated and observed spectra in the first domain. For a better comparison with the experimental data, a scaling factor of 0.975 has been used in order to take into account the harmonic character of the calculated frequencies. This factor has been chosen to get the best fit between observed and calculated values. For the anti−anti form the calculations predict (lower trace of Figure 1) the presence of two main bands at about 1300 and 1240 cm^{-1}, assignable to the COH bending modes of PD and PA, respectively; other

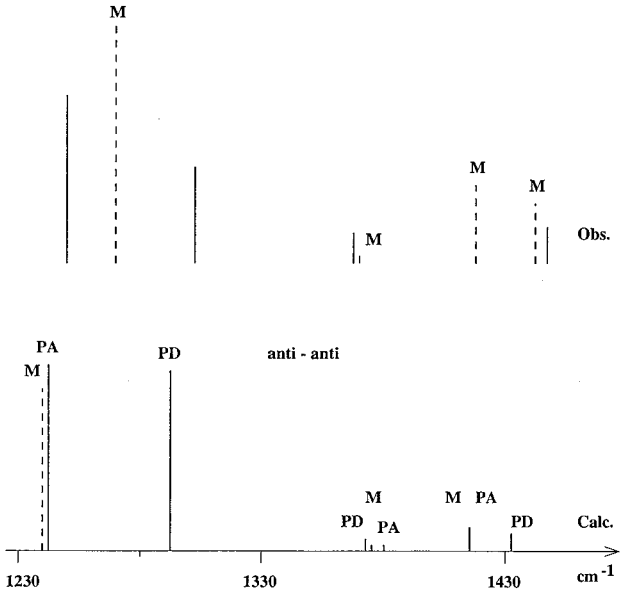

Figure 2. Bar infrared spectrum in the range 1440−1230 cm^{-1} of ethanol monomer and dimer in their anti conformation. Lower trace, calculated (scaling factor for the frequencies, 0.975); upper trace, observed for species C in argon matrix.

features, at least four times weaker, are located above 1370 cm^{-1}. For the gauche−gauche form (lower trace of Figure 3), the two main bands are located around 1400 cm^{-1}, the COH bending being strongly coupled with the methyl symmetric bending and the methylene wagging motions.

The region 1100−1020 cm^{-1} also discriminates the anti or gauche character of PA and PD. Two clear-cut situations are displayed in Figures 4 and 5; the first one, anti−anti, is characterized by two strong bands below 1050 cm^{-1} and two weaker signals at 1100 ± 15 cm^{-1}. In the second situation, gauche−gauche, the two strongest bands are located above 1070

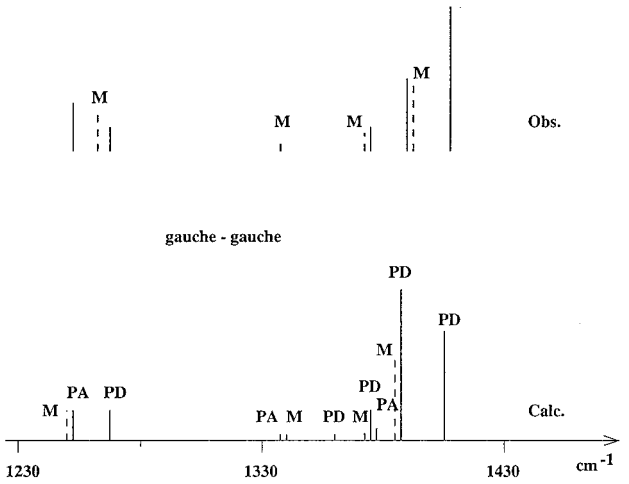

Figure 3. Bar infrared spectrum in the range 1440−1230 cm^{-1} of ethanol monomer and dimer in their gauche conformation. Lower trace, calculated (scaling factor for the frequencies, 0.975); upper trace, observed for species F in argon matrix.

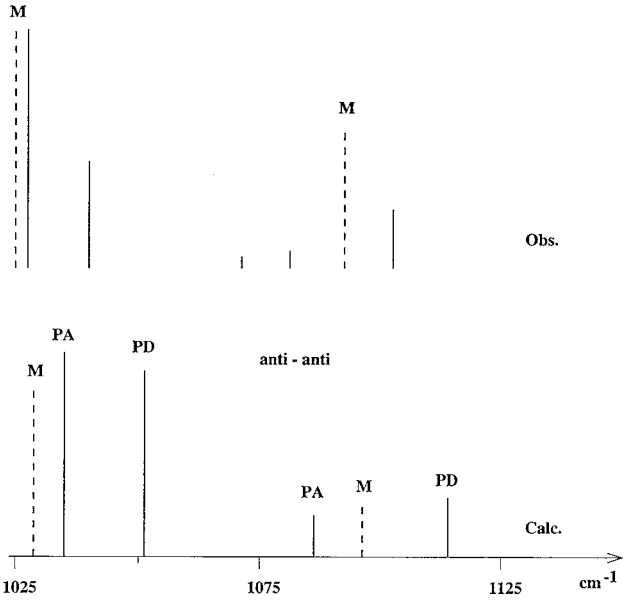

Figure 4. Bar infrared spectrum in the range 1120−1020 cm^{-1} of ethanol monomer and dimer in their anti conformation. Lower trace, calculated; upper trace, observed for species C in argon matrix.

cm^{-1}, the two others, 20% weaker, in the range 1060−1050 cm^{-1}. These differences would be expected if one recalls the noticeable spectral changes from anti- to gauche-ethanol monomer,[6] the anti form being characterized by two bands at 1095 and 1029 cm^{-1} (the first one three times weaker) and the gauche form by two bands at 1068 and 1056 cm^{-1} (the first one three times stronger). Unfortunately the situation is rendered complicated for the anti−gauche form because of a surprising coupling between the CCO motions of the two partners, giving rise to two nearly degenerate modes at 1050 cm^{-1}.

As for the region 800 cm^{-1}, Figure 6 displays the remarkable behavior of the methylene rocking (rCH_2) mode characterized by a higher frequency and a much lower intensity for the anti form of both PA and PD. Typically the anti/gauche frequency shift is of about 15 cm^{-1} and the intensity ratio at least a factor of 10. Such a difference stems from a weak coupling between the CH_2 rocking and the CO stretching in the case of the gauche form.

To conclude this vibrational analysis, it appears that the anti character of PD is identified by two strong bands around 1300

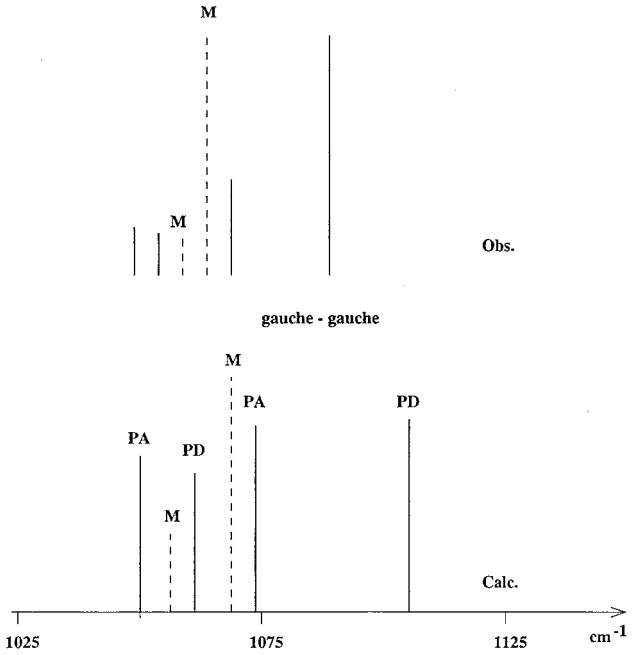

Figure 5. Bar infrared spectrum in the range 1120−1020 cm^{-1} of ethanol monomer and dimer in their gauche conformation. Lower trace, calculated; upper trace, observed for species F in argon matrix.

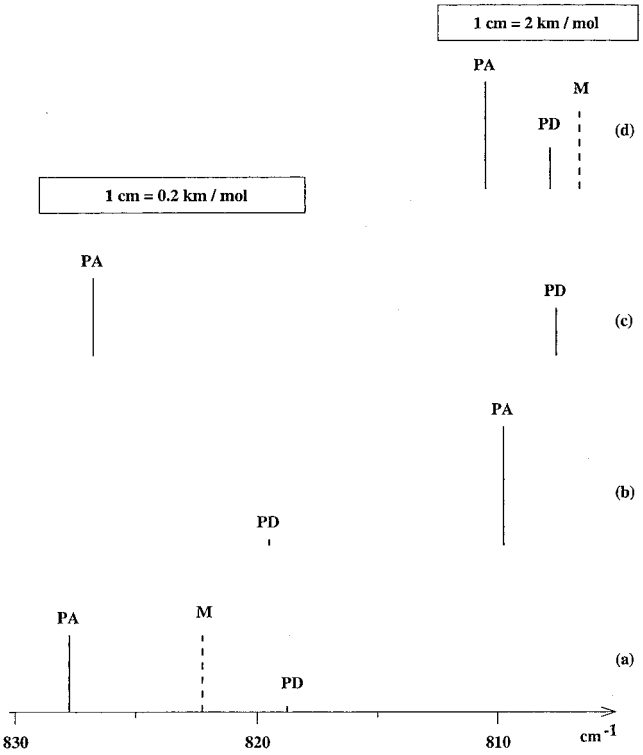

Figure 6. Calculated bar spectra of the methylene rocking modes of ethanol dimer in its four stable conformations anti−anti (a), anti−gauche (b), gauche−anti (c), and gauche−gauche (d). Note the change in intensity scale from *anti*- (830−815 cm^{-1}) to *gauche* (810−800 cm^{-1}) -ethanol.

and 1040 cm^{-1}, that of PA by two strong bands around 1250 and 1030 cm^{-1}; on the other hand, the gauche character of PD is identified by two strong signals around 1400 and 1100 cm^{-1}, that of PA by one strong band close to 1060 cm^{-1}. Furthermore the presence of gauche forms for PA and/or PD is confirmed by the presence of rCH_2 signals around 800 cm^{-1}, that of anti forms by the observation of weak bands around 810 cm^{-1}.

TABLE 4: Vibrational Frequencies (cm^{-1})[a] of Ethanol Dimers Trapped in Argon Matrix at 7 K

	$\nu_{irr} = 3527\ cm^{-1}$ [b]		$\nu_{irr} = 3536\ cm^{-1}$ [c]		
$(C_2H_5OH)_2/Ar$[a]	C	F	A	E	assignment
3665.3 w			3665.4 m		PA νOH
3660.1 w	3660.4 m	3646.0 m			
3536.2 s			3536.2 s	3520.7 s	
3531.2 s					PD νOH
3527.2 s	3527.2 s	3506.6 s			
3523.3 s					
2988.3	2987.7 m	2996.7 m			νCH_3, νCH_2
	2984.1 m				
2977 b, m	2977.6 w	2972.8 m			
	2938.8				
	2906.8 w				
	2901.4 m				
1491 b, w	1491.1 w	1484.7 w			δCH_2
	1446.3 w	1449.5 m			δCH_3 + wCH_2
	1443.8 w				
	1436.3 w			1433.5 w	
		1404.7 m		1399.0 m	
		1391.4 m			
1368.2 w	1368.3 w	1373.3 w			
1308.3 m					
1302.4 m	1302.3 m	1267.8 w	1309.0 m	1300.8 w	PD δOH
				1291.5 w	PA δOH
1243.7 m	1241.8 m	1250.8 w	1243.1 s		
			1235.9 w	1238.5 w	
	1163.0 w				rCH_3
	1159.5 w	1129.0 w			
1102.5 m	1102.4 m			1099.3 w	PD rCH_3 + ν_aCCO
1083.6 w	1082.1 w	1087.6 b, m	1083.6 m	1071.9 w	
		1068.2 b, w			PA rCH_3 + ν_aCCO
1044.1 m					
1039.2 m	1039.1 s	1053.9 m	1057.5 m	1061.7 m	PD ν_aCCO + rCH_3
1027.4 m	1027.4 s	1049.3 m	1046.1 m	1040.6 m	PA ν_aCCO + rCH_3
888.9 w	888.9 m	877.4 m	890.5 m		PD ν_sCCO
884.6 m	884.5 m	873.7 m	886.6 w	879.8 m	PA ν_sCCO
	812.6 w	800.8 m		802.4 w	rCH_2 + rCH_3
	809.2 w				

[a] Bands identified from annealing and concentration effects: s, strong; m, medium; w, weak; b, broad. [b] Bands whose intensity decreases (C) or increases (F) upon irradiation at 3527 cm^{-1}. [c] Bands whose intensity decreases (A) or increases (E) upon irradiation at 3536 cm^{-1}.

IV. Spectral Results

In argon as well as in nitrogen matrix the vibrational spectrum of $(C_2H_5OH)_2$, as obtained after deposition or annealing of diluted samples, is remarkably intricate owing to the large number of bands attributable to it in each spectral region. The identification of several species was, however, rendered possible by selective infrared irradiations giving rise to more or less complete conversion of the excited species into one or several other forms. The data obtained in argon, whose interpretation is quite simple for the main species, will be first reported and analyzed. Those relating to nitrogen matrix will described in a second part.

IV.A. Results in Argon. *IV.A.1. Concentration and Annealing Effects.* Careful concentration and annealing effects were examined in Paris. The concentration range explored, 1/300 to 1/3000, was large enough to identify many dimer bands after sample deposition, in nearly complete absence of larger polymers. On the other hand, annealing of diluted samples enabled the aggregation state to be limited essentially to the dimer. These two complementary approaches led thus to a good definition of the dimer spectrum. The left column of Table 4 gathers the results of these experiments, which deserve the following comments. The identification of two kinds of νOH bands, one with frequencies close to that the monomer and the other about 130 cm^{-1} red shifted proves that the dimer is open chain, the first group being assigned to PA, the second to PD. The presence of multiplets in each region suggests the existence of several conformers. For convenience the species absorbing at 3536.2, 3531.2, 3527.2, and 3523.3 cm^{-1} will be referred to as species A, B, C, and D, respectively. C predominates after deposition so that most of the dimer bands identified in the other spectral regions in the same conditions have to be associated to this species. The most important domain for conformational analysis, 1350−1200 cm^{-1}, displays two bands at 1302.4 and 1243.7 cm^{-1}, the first one being one of the strongest dimeric signals. In the νCCO + rCH_3 domain, 1100−870 cm^{-1}, three groups of bands are observed: 1102.5−1082.4, 1039.2−1027.4, and 888.9−884.6 cm^{-1}. The positions of three groups of bands remarkably parallel those of the anti form of the monomer. On one hand, the doublet 1302.4−1243.7 cm^{-1}, correlated to the strong monomer band at 1239.5 cm^{-1}, is assignable to δOH of PD and PA, respectively. The large blue shift (63 cm^{-1}) for PD is a well-known effect of hydrogen bonding on the δOH mode.[16] On the other hand, the doublets 1102.5−1082.4 and 1039.2−1027.4 cm^{-1} are close to the anti monomeric bands at 1091.7 and 1025.0 cm^{-1} assigned to νCCO + rCH_3. The fourth doublet 888.9−884.6 cm^{-1} is not significant since both anti and gauche forms absorb at about 886 cm^{-1}. These observations gathered in Table 6 and compared to the results of calculations are thus strong support for assignment of species C to a dimer in which both PA and PD subunits are anti conformers. They are also in line with the fact that *anti*-ethanol is the only monomeric form present in solid argon.[6] It is worth noting that the depletion spectra[7] of ethanol dimer, either in the gas phase

TABLE 5: Interconversion between Conformers of Ethanol Dimer Trapped at 7.6 K in Solid Argon or Nitrogen upon Selective Irradiation at ν_{irr} (cm^{-1})[a]

Argon matrix

$$\underline{A}\ (3536.2) + C\ (3527.2) \xrightarrow{\nu_{irr} = 3536} \underline{E}\ (3520.7) + F\ (3506.6)$$

$$B\ (3531.2) + \underline{C} \xrightarrow{\nu_{irr} = 3531} G\ (3513.5) + \underline{F}$$

$$C \xrightarrow{\nu_{irr} = 3527} F$$

Nitrogen Matrix[b]

$$\alpha\ (3516.5) \xrightarrow{\nu_{irr} = 3516.5} \underline{\beta_1}\ (3502.5) + \beta_2\ (3500.0)$$

$$\underline{\beta_1} + \beta_2 \xrightarrow{\nu_{irr} = 3502} \underline{\alpha} + \epsilon\ (3486.2) + \eta\ (3477.4)$$

$$\beta \xrightarrow{\nu_{irr} = 3500} \underline{\alpha} + \epsilon + \eta$$

$$\underline{\delta}\ (3489.8) + \epsilon \xrightarrow{\nu_{irr} = 3487} \beta + \alpha$$

$$\eta\ (3477.4) \xrightarrow{\nu_{irr} = 3487} \delta + \beta$$

$$\underline{\zeta}\ (3470.3) + \eta \xrightarrow{\nu_{irr} = 3470} \underline{\alpha} + d\alpha + \beta$$

[a] In cases where several conformers are involved in conversions at the same irradiation frequency, the species participating into the main process are underlined. The PD νOH frequency (cm^{-1}) of each conformer is given in parentheses. [b] When both β_1 and β_2 behave in the same way they are referred to as β.

TABLE 6: Comparison between Calculated and Observed Shifts $\Delta\nu = \nu_{dimer} - \nu_{monomer}$ (cm^{-1}) of the Most Significant Vibrational Modes of *anti*−*anti*-(C_2H_5OH)$_2$

	Anti−Anti			
	calcd		obsvd[a]	
	PD	PA	PD	PA
νOH	−163.6	−7.4	−128.4	4.8
δOH	57.1	5.6	62.8	2.3
rCH_3	1.0	2.9	−1.5	2.0
$rCH_3 + \nu_aCCO$	17.1	−9.3	10.7	−9.6
$\nu_aCCO + rCH_3$	21.2	6.0	14.2	2.4
ν_sCCO	3.7	−5.7	1.0	−3.4
$rCH_2 + rCH_3$	−3.3	5.4	−2.6	0.8

[a] Species C in argon at 7 K. Monomer values taken from ref 6.

or adsorbed on large argon clusters, limited to the regions 1100−1020 and 910−870 cm^{-1}, show some analogies with these matrix data. In the first region the two main bands at 1045.4−1031.4 cm^{-1} (free dimer), red shifted to 1043.9−1029.7 cm^{-1} (adsorbed dimer), correspond to the strong matrix doublet 1037.2−1027.4 cm^{-1}, but the weaker features in the range 1080−1060 cm^{-1} have no equivalence in the matrix spectra. It is probable that this band multiplicity stems from the presence of several conformers, but the absence of data in the region 1400−1200 cm^{-1} makes the discussion inconclusive.

IV.A.2. Monochromatic Irradiations. OPO irradiations were carried out at each of the PD νOH frequencies of A, B, C, and D species. The experiments were performed at 7.6 K on annealed samples with Ar/C_2H_5OH molar ratios of the order of 500. Irradiation at 3527 cm^{-1} (excitation of C) led to a specific interconversion process. On the contrary, irradiations at A, B, or D frequencies led to complicated conversion schemes, two species at least disappearing concomitantly (Table 5). Between two irradiation cycles the sample was regenerated by warming to 12 K for 5 min. The fast back-conversion processes prompted us to study their kinetics in the dark in the temperature range 7−18 K. They will be reported at the end of this section.

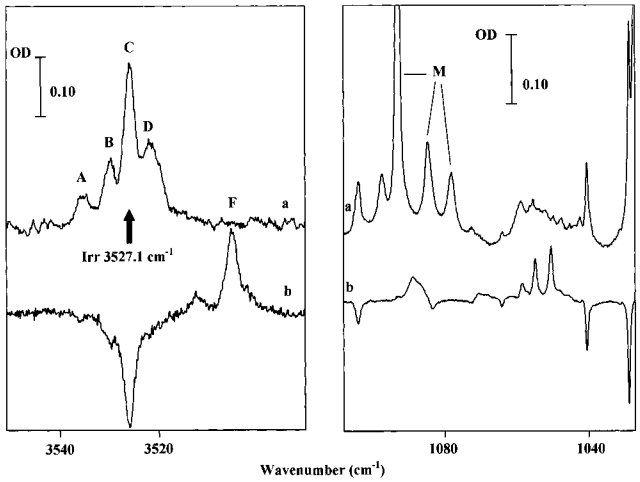

Figure 7. Effect of irradiation at 3527 cm^{-1} on a Ar/C_2H_5OH = 514 sample annealed to 38 K. Spectra recorded at 7.6 K. Upper traces, before irradiation; lower traces, difference spectrum after subtraction before 12 min irradiation (laser power, 28 mW).

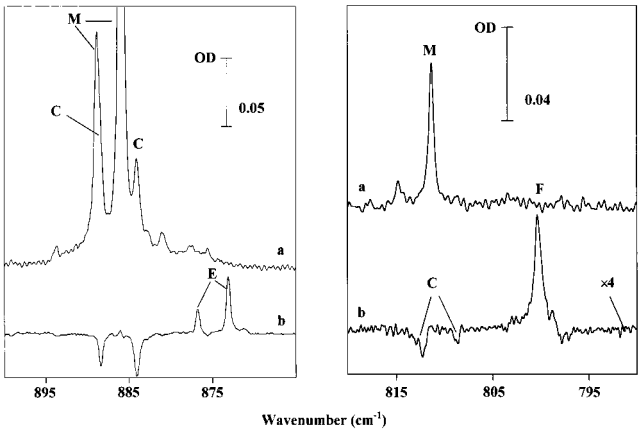

Figure 8. Same caption as for Figure 7.

Irradiation at 3527 cm^{-1}. After 1 min irradiation at 3527 cm^{-1} (Figure 7) about 75% of C has been converted into another species labeled F characterized by two νOH bands at 3646.0 and 3506.6 cm^{-1}. Table 4 gathers the frequencies of the bands whose intensity decreases (species C) or increases (species F) during the irradiation cycle. Many C bands had already been identified in concentration/annealing experiments (vide supra). Those that are weak or overlap absorptions due to other species are better identified in the difference spectra after subtraction before irradiation. In particular the observation of weak bands in the range 1430−1350 cm^{-1} confirms the structure as anti−anti. Indeed it is clear, from the schemes displayed in Figure 2, that the calculated spectrum for such a structure, characterized by two main bands around 1300 and 1240 cm^{-1} and much weaker features above 1350 cm^{-1}, correctly fits the observed spectrum, unlike the calculated gauche−gauche one in which the main signals are located above 1380 cm^{-1} (Figure 3).

Species F, not present before irradiation, is also an open chain dimer whose spectrum is well-identified below 1430 cm^{-1}. The absence of strong bands around 1245 and 1030 cm^{-1} excludes the anti structure for PA; the absence of strong bands close to 1300 cm^{-1} and the localization around 1400 cm^{-1} of the main bands in the domain 1430−1230 cm^{-1} (Figure 3) suggest a gauche structure for PD; thus one concludes that F has a gauche−gauche structure. The difference spectrum in the range 820−790 cm^{-1} displayed in Figure 8 clearly shows the red shift and the intensification of the CH_2 rocking band from anti to

gauche conformation predicted by the calculations (Figure 6). However, only one signal at 800.9 cm^{-1} is observed for F instead of the two expected. A possible explanation is an overlap of the two bands, the observed signal being broadened on its low-frequency side.

Irradiation at 3536 cm^{-1}. Irradiation at 3536 cm^{-1} induces conversion of both A and C species because of band overlap and of the high photosensitivity of C. The generated species are F (coming from C) and a new one, hereafter referred to as E, characterized by a PD νOH band at 3520.7 cm^{-1}. The identified bands of A and E are reported in Table 4. The strongest bands of A in the domain 1430−1230 cm^{-1} are located at 1309 and 1243 cm^{-1}, which suggests an anti−anti structure. However, the situation is not so clear in the range 1100−1030 cm^{-1} where the main bands are located at about 1084, 1057, and 1046 cm^{-1}. As for species E, the presence of at last one partner with a gauche form is deduced from the presence of a strong band at 1399 cm^{-1}, in partial overlap with the bands of species F at 1405−1391 cm^{-1}, and by a noticeable narrow feature at 802.4 cm^{-1} in the absence of any signal of its precursor in the same domain.

Irradiation at 3523 cm^{-1}. The main spectral changes upon irradiation at 3523 cm^{-1} correspond to the C → F conversion because of band overlap. Secondary effects corresponding to the intensity decrease of D are hardly observable, and in any case do not allow one to conclude about the conformation of this species.

Irradiation at 3531 cm^{-1}. A complicated photoconversion scheme occurs upon irradiation at the PD νOH frequency of species B. The main process is C → F, followed by the conversion of B into another species absorbing at 3513.5 cm^{-1} and, to a less extent, of A into E. Band overlap makes difficult the identification of the bands of B. As for its descendant, it is characterized by four features at 3513.5, 1291.8, 1057.0, and 882.2 cm^{-1}.

Back-conversion in the Dark. The C ← F back-conversion in the dark has been studied at three temperatures (7.6, 13.0, and 17.0 K) according to the following method. After one irradiation cycle the sample was kept in the dark, and spectra limited to the region 1200−550 cm^{-1} by means of an interference filter were recorded for about 20 min. This duration was long enough for the sample to recover its spectrum before irradiation. The C ← F conversion was followed by measuring the intensities of the bands at 1049.3 and 1027.4 cm^{-1}, respectively assigned to F and C. The data analysis was carried out under the hypothesis of a first-order process characterized by a kinetic rate constant k_T such as

$$\frac{d[C]}{dt} = -\frac{d[F]}{dt} = k_T[F]$$

Integration of these equations leads to

$$[F] = [F]_0 \exp(-k_T t) \text{ and } \frac{[C]_\infty - [C]}{[C]_\infty - [C]_0} = \exp(-k_T t).$$

Logarithmic plots of these relationships are linear with slopes equal to −0.0018, −0.0028, and −0.0043 s^{-1} at 7.6, 13, and 17 K, respectively. An Arrhenius plot ln k_T versus T^{-1} leads to an activation energy of the order of 100 J mol^{-1}.

IV.B. Results in Nitrogen. *IV.B.1. Annealing Effect.* Several species of dimer were differentiated according to their growth rate dependence with the annealing temperature. However, their identification was complicated to some extent by the simultaneous thermal conversion anti → gauche of the monomer.[6]

Annealing to 26 K of relatively concentrated samples (N_2/C_2H_5OH = 300−500) leads to the formation of not less than seven dimeric species characterized by νOH PD frequencies at 3516.5, 3502−3500 (overlapping doublet), 3494.1, 3489.7, 3486.2, 3477.4, and 3470.3 cm^{-1}. These species will be referred to as α, β, γ, δ, ϵ, η, ζ in the order of decreasing frequencies. A second annealing to 30 K causes the growth of α and, to a much less extent, of ϵ and the decrease of γ. The whole spectrum of α, which becomes the predominant species, can then be identified (Table 7). A remarkable point is that α is characterized in the free OH stretching domain by three bands with comparable intensities at 3646.0, 3641.8, and 3636.7 cm^{-1}. Such a multiplicity suggests that there exists several subclasses of α differing by the conformation of PA.

IV.B.2. Monochromatic Irradiations. OPO irradiations were carried out at each of the νOH absorption frequencies previously reported for the PD molecule of the various dimers. The experiments were done at 7.6 K on annealed samples with N_2/C_2H_5OH molar ratios of the order of 350. Positive effects were obtained at each frequency, as shown in Figure 8, which displays the effects of successive irradiations at 3516, 3500, and 3487 cm^{-1}. The analysis of the photoconversions was revealed to be difficult because of band overlap causing the simultaneous conversion of several precursors and because of the formation of several products from one precursor (Table 5). The only way to analyze correctly the processes was to record spectra after short irradiation durations, of the order of some tens of seconds, to follow the different steps of conversion occurring at different time scales.

Irradiation at 3516.5 cm^{-1}. After 1 min irradiation at 3516.5 cm^{-1}, the corresponding band assigned to the α dimeric species has been reduced to about a quarter of its initial intensity, with concomitant intensity increase of the β doublet close to 3500 cm^{-1}, and, to a much less extent, of the γ signal at 3494.1 cm^{-1} (Figure 10). Longer irradiation times give rise to an interesting process, the β component at 3502.5 cm^{-1} (hereafter referred to as β_1) decreasing in intensity, the other (β_2), at 3500 cm^{-1}, continuing to grow. This opposite behavior of β_1 and β_2 enables their spectra to be separately identified (Table 7). Furthermore the decrease of β_1 correlates with the growth of the δ bands. The structural properties of α stem from the following observations. In the range 1430−1240 cm^{-1} the main band is located at 1305 cm^{-1}, typical of the PD δOH mode of *anti*-ethanol (1302.3 cm^{-1} for species C in argon). The anti character of PD is confirmed by the strong bands at 1100.2 and 1040 cm^{-1} (ν_aCCO + rCH_3). Accordingly the doublet 1063.4−1055.9 cm^{-1} should be assigned to the two modes (rCH_3 + ν_aCCO) of PA measured at about the same frequencies for monomeric *gauche*-ethanol, the intensity of the high-frequency component being in both cases three to four times stronger. It is thus concluded that α is an anti−gauche dimer. However, this conclusion does not agree with the calculations that predict two quasi degenerate modes at 1050 cm^{-1} involving simultaneous motions of both moieties; such an intermolecular coupling, exclusively obtained for these two modes of the anti−gauche conformer, casts some doubt on the quality of the calculated values.

Irradiation at 3502 cm^{-1}. In the first 3 min of irradiation at 3502 cm^{-1} the β_1 component centered at 3502.5 cm^{-1} strongly decreases in intensity, while the low-frequency component β_2 is weakly modified. For longer durations of irradiation, this second component tends to decrease significantly. The main product of photolysis is α in both cases, but the ϵ and η species, absorbing at 3486 and 3477.1 cm^{-1}, respectively, also grow up. The assignment of β_1 deduced from the band intensity

TABLE 7: Vibrational Frequencies (cm^{-1})[a] of Ethanol Dimers Trapped in Nitrogen Matrix at 7 K

annealing[b]	α[c]	β_1[d]	β_2[e]	δ[f]	η[g]	ζ[h]
3646.0 w	3646.0 w	3653.5 w	3635.0 w	3639.2 w		3637.0 w
3641.8 w	3641.7 w					
3636.7 w						
3516.5 s	3516.5 s	3502.5 s	3500.5 s	3489.8 s	3477.4 s	3470.3 s
3501 w, b						
3490 w						
1445.0 w	1445.0 w					
	1438.3 w, b					
					1414.0 w, b	
1399.9 w	1399.7 m		1398.3 w			
1397.0 w	1397.0 w		1395.5 w	1392.0 w, b	1394.1 w	
1370.4 w	1370.5 w	1369.0 w	1373.3 w	1372.7 w		1372.5 w
		1345.0 w	1340.4 w	1346.4 w		
1314.5 w	1314.5 w		1317.6 m	1317.9 w	1322.5 w	1322.2 w
1304.3 m, b	1305.6 m		1307.7 m	1312.0 w	1314.9 w	1315.8 w
	1304.2					
1268.6 w		1278.2 w		1274.5 w		1275.2 w
	1258.3 w	1257.1 w	1252.5 w			
	1121.2 w					
1100.2 m	1100.1 s	1107.4 w	1102.0 m, b	1102.6 w	1104.3 w	1097.0 w
1082.1 w				1085.2 w	1084.5 w, b	1084.2 w
1074.5 w, b		1072.5 w				
1063.4 m	1063.4 s	1065.4 w	1060.5 w			
1056.0 m	1055.9 w		1057.2 s	1057.3 m		1051.9 m
1051.9 m		1051.8 s		1050.3 m	1048.2 m, b	1047.9 m
1048.9 m, b		1048.7 w				
1041.5 w						
1040.6 s	1040.7 s		1043.3 s, b			
1039.7 s	1039.8	1031.8 w			1029.2 w	1029.5 w
888.8 w	888.7 w	891.8 w	888.6 w	896.5 w		
882.9 m	882.9 m	877.7 m	883.3 w, b	876.7 w	874.5 w	876.4 w
						874.8 w
812.5 w	812.5 w		811.5 w			801.9 w
808.8 w, b	808.9 w	800.3 w	808.3 w	799.7 w	800.7 w	799.9 w
596.5 m	596.5 m					

[a] The bands in the spectral range 3000−1450 cm^{-1} have not been reported: s, strong; m, medium; w, weak; b, broad. [b] Bands growing preponderantly in the temperature range 28−30 K. [c] Bands whose intensity decreases upon irradiation at 3516 cm^{-1}. [d] Bands whose intensity decreases upon irradiation at 3502 cm^{-1}. [e] Bands whose intensity decreases upon irradiation at 3500 cm^{-1}. [f] Bands whose intensity decreases upon irradiation at 3487 cm^{-1}. [g] Bands whose intensity decreases upon irradiation at 3478 cm^{-1}. [h] Bands whose intensity decreases upon irradiation at 3470 cm^{-1}.

decreases at the beginning of irradiation at 3502 cm^{-1} confirms the one deduced from the effect of irradiation at 3516 cm^{-1}. In the absence of any characteristic band in the domain 1430−1240 cm^{-1}, the structure of β_1 cannot be specified.

Irradiation at 3500 cm⁻¹. Irradiation at 3500 cm^{-1} induces the photoconversion of both β_1 and β_2 species, the main product being α, species ϵ and η growing moderately. The observed spectral changes confirm the assignment already proposed for β_2. The structure of this species can be discussed on the following grounds: the main bands in the range 1430−1240 cm^{-1} are located around 1310 cm^{-1}, which is typical of an anti form for PD. This structure is compatible with the presence of the bands at 1102.0 (medium) and 1043.3 (strong) cm^{-1}. For PA we suggest a gauche structure characterized by a strong signal at 1057.2 cm^{-1}.

Irradiation at 3487 cm⁻¹. Two species at the origin of the overlapping bands at 3489.8 and 3486.0 cm^{-1} are affected by irradiation at 3487 cm^{-1}. In the first 2 min of irradiation the broader component at 3489.8 cm^{-1} (corresponding to species δ) strongly decreases in intensity, the 3486.0 cm^{-1} component (associated with η) being weakly modified. Then, for longer durations of irradiation, both species are converted in the same proportions. The species generated during these different steps are $\beta_1 + \beta_2$ and, to a less extent, α. Table 7 gathers the bands of δ identified at the beginning of the irradiation cycle. Those assignable to ϵ are scarce and located below 1100 cm^{-1} (1082.2, 1064.5, 1049.1, and 874.6 cm^{-1}).

Irradiation at 3478 cm⁻¹. One minute irradiation at 3478 cm^{-1} causes a 50% intensity decrease of the band centered at 3477 cm^{-1} characterizing species η and an increase of the bands at 3497.8 and 3489.8 cm^{-1}. Table 7 reports the frequencies of the bands assignable to η on the basis of their intensity decrease.

Irradiation at 3470 cm⁻¹. In the first step of irradiation, which lasts about 1 min only species ζ absorbing at the irradiation frequency decreases in intensity with concomitant increase of the bands assigned to α. For longer irradiation duration, η is also photolyzed, probably because of band overlap. Table 7 gathers the frequencies of the band of ζ assignable on the basis of their intensity decrease at the beginning of the irradiation cycle.

Back-conversions in the Dark. The behavior of the photoproducts after irradiation at 3516.5, 3500, and 3478 cm^{-1} was studied at 7.6 K under the same conditions as in argon matrix. In each case the back-conversions are very slow and, as a consequence, have not been examined in detail. In the case of the photoconversion of α upon irradiation at 3516.5 cm^{-1}, less than 10% s of the converted quantity of α was regenerated after 40 min in the dark, with concomitant decrease of the β_2 concentration. The same proportion of β_2 was regenerated in 40 min after photolysis at 3500 cm^{-1}. Lastly, in the case η photolyzed at 3478 cm^{-1}, about 20% was regenerated after 30 min in the dark.

V. Conclusion

The dimer of ethanol is trapped in argon or nitrogen matrices under several open chain conformers readily interconverted upon

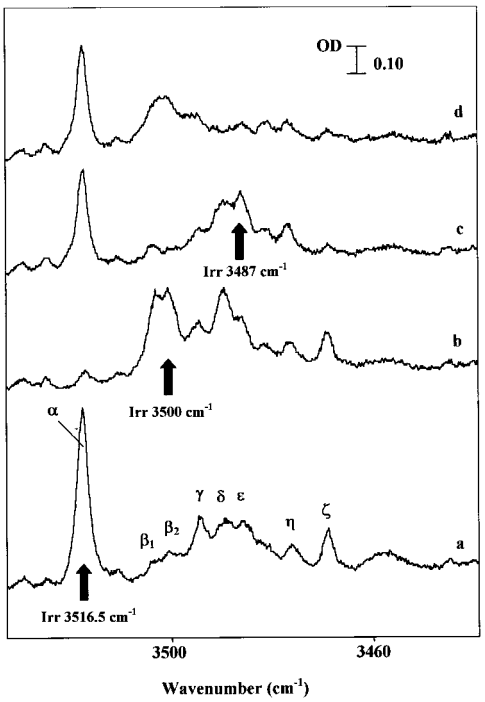

Figure 9. Effects of successive irradiations for a $N_2/C_2H_5OH = 450$ samples annealed to 29 K. Recording temperature, 7.6 K. (a) Before irradiation; (b) after 15 min irradiation at 3516.5 cm^{-1} (laser power, 22 mW); (c) after 8 min irradiation at 3500 cm^{-1} (laser power, 6 mW); (d) after 8 min irradiation at 3487 cm^{-1} (laser power, 5 mW).

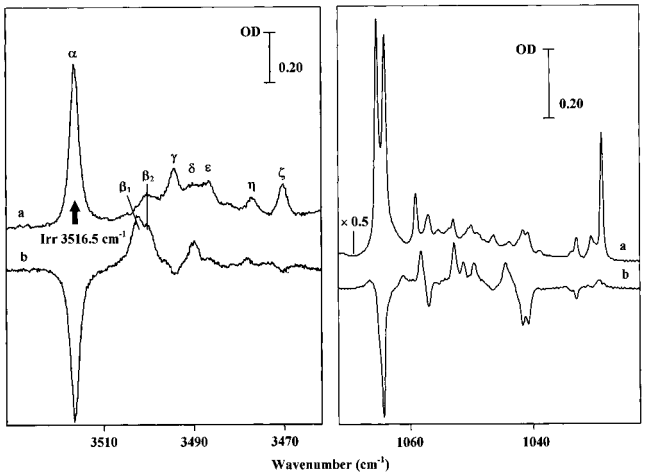

Figure 10. Effects of irradiation at 3516.5 cm^{-1} for a $N_2/C_2H_5OH = 450$ sample annealed to 29 K. Recording temperature, 7.6 K.

excitation of their PD νOH mode. The band intensity decrease or increase during irradiation cycles allows a nearly complete assignment to be proposed for some of them. Quantum chemistry calculations predict the presence of several minima in the potential energy surface with comparable energies but very different vibrational spectra according to the trans or gauche character of the two partners. Specific trans/gauche vibrational fingerprints allow the trans−trans conformer to be identified as the predominant species in argon, with δOH and ν_aCCO modes close to 1300−1040 and 1240−1030 cm^{-1} for PD and PA, respectively, while its gauche−gauche photoproduct is characterized by three doublets centered at about 1400, 1075, and 1050 cm^{-1}. The relative stability of the conformers is dependent on the nature of the matrix since in nitrogen the most abundant conformer is anti−gauche (main bands at 1300−1040 cm^{-1} for PD and 1400−1060 cm^{-1} for PA). The weak energy gaps between these conformers are at the origin of such matrix effects, already observed for the methanol−water heterodimer.[18,19] Similarly, as previously observed for $(CH_3OH)_2$, the products of photolysis are better stabilized in nitrogen than in argon, possibly because of a specific interaction between the free OH group of PA and one molecule of the host crystal. Coming after the photolysis of methanol aggregates according to the same technique of selective infrared irradiation in the 2.8 μm region, this study confirms the high photosensitivity of clusters of alcohols in matrix as well as in liquid[20−24] or gas phase.[7]

Acknowledgment. The authors thank Professor S. Leutwyler and the supercomputer center of the University of Bern who supported the theoretical part of this work. The authors thank also Dr. V. Brenner for her grateful advice.

References and Notes

(1) Bakkas, N.; Loutellier, A.; Racine, S.; Perchard, J. P. *J. Chim. Phys.* **1993**, *90*, 1703.
(2) Bakkas, N.; Bouteiller, Y.; Loutellier, A.; Perchard, J. P.; Racine, S. *J. Chem. Phys.* **1993**, *99*, 3335.
(3) Coussan, S.; Loutellier, A.; Perchard, J. P.; Racine, S.; Peremans, A.; Tadjeddine, A.; Zheng, W. Q. *J. Chem. Phys.* **1997**, *107*, 6526.
(4) Coussan, S.; Bouteiller, Y.; Loutellier, A.; Perchard, J. P.; Racine, S.; Peremans, A.; Tadjeddine, A.; Zheng, W. Q. *Chem. Phys.* **1997**, *219*, 221.
(5) Coussan, S.; Loutellier, A.; Perchard, J. P.; Racine, S.; Peremans, A.; Tadjeddine, A.; Zheng, W. Q. *Chem. Phys.* **1997**, *223*, 279.
(6) Coussan, S.; Bouteiller, Y.; Perchard, J. P.; Zheng, W. Q. *J. Phys. Chem. A* **1998**, *102*, 5789.
(7) Ehbrecht, M.; Huisken, F. *J. Phys. Chem. A* **1997**, *101*, 7768.
(8) Kieninger, M.; Suhai, S. *Int. J. Quantum Chem.* **1994**, *52*, 465.
(9) Gonzáles, L.; Mó, O.; Yáñez, M.; Elguero, J. *J. Mol. Struct.: THEOCHEM* **1996**, *371*, 1.
(10) Mó, O.; Yáñez, M.; Elguero, J. *J. Chem. Phys.* **1997**, *107*, 3592.
(11) Hagemeister, F. C.; Gruenloh, C. J.; Zwier, T. S. *J. Phys. Chem. A* **1998**, *102*, 82.
(12) Gonzáles, L.; Mó, O.; Yáñez, M. *J. Chem. Phys.* **1998**, *109*, 139.
(13) Gonzáles, L.; Mó, O.; Yáñez, M. *J. Chem. Phys.* **1999**, *111*, 3855.
(14) Frish, M. J.; Trucks, G. W.; Schlegel, H. B.; Gill, P. M. W.; Jonhson, B. G.; Womg, M. W.; Foresman, J. B.; Robb, M. A.; Head-Gordon, M.; Replogle, E. S.; Gomperts, R.; Andres, J. L.; Raghavachari, K.; Binkley, J. S.; Gonzalez, R. L.; Martin, R. L.; Fox, D. J.; Defrees, D. J.; Baker, J.; Stewart, J. J. P.; Pople, J. A. *GAUSSIAN*, Revision D. 4; Gaussian: Pittsburgh, PA, 1995.
(15) Becke, A. D. *J. Chem. Phys.* **1993**, *98*, 5648. Lee, C.; Wang, W.; Parr, R. G. *Phys. Rev. B* **1988**, *37*, 785.
(16) Asselin, M.; Sandorfy, C. *Can. J. Chem.* **1971**, *49*, 1539.
(17) Barnes, A. J.; Hallam, H. E. *Trans. Faraday Soc.* **1970**, *66*, 1932.
(18) Bakkas, N.; Bouteiller, Y.; Loutellier, A.; Perchard, J. P.; Racine, S.; *J. Chem. Phys.* **1993**, *99*, 3335.
(19) Bakkas, N.; Bouteiller, Y.; Loutellier, A.; Perchard, J. P.; Racine, S. *Chem. Phys. Lett.* **1995**, *232*, 90.
(20) Graener, H.; Ye, T. Q.; Laubereau, A.; *J. Chem. Phys.* **1989**, *90*, 3413.
(21) Laenen, R.; Rauscher, C. *J. Chem. Phys.* **1997**, *106*, 8974.
(22) Laenen, R.; Rauscher, C.; Laubereau, A. *Chem. Phys. Lett.* **1998**, *283*, 7.
(23) Laenen, R.; Rauscher, C. *J. Mol. Struct.* **1998**, *448*, 115.
(24) Laenen, R.; Simeonidis, K. *Chem. Phys. Lett.* **1998**, *292*, 631.